A REVIEW OF DYNAMIC INFLOW
AND ITS EFFECT ON EXPERIMENTAL CORRELATIONS

Gopal H. Gaonkar
Professor
Department of Aeronautical Engineering
Indian Institute of Science
Bangalore, INDIA   56-0012

and

David A. Peters
Professor and Chairman
Department of Mechanical Engineering
Washington University
St. Louis, Missouri   63130

Abstract

A review is given of the relationship between experimental data and the development of modern dynamic-inflow theory. Some of the most interesting data, first presented 10 years ago at the Dynamic Specialists' Meeting, is now reviewed in light of the newer theories. These pure blade-flapping data correlate very well with analyses that include the new dynamic inflow theory, thus verifying the theory. Experimental data are also presented for damping with coupled inplane and body motions. Although inclusion of dynamic inflow is often required to correlate this coupled data, the data cannot be used to verify any particular dynamic inflow theory due to the uncertainties in modeling the inplane degree of freedom. For verification, pure flapping is required. However, the coupled data do show that inflow is often important in such computations.

Notation

a	slope of lift curve, rad^{-1}
B	tip loss factor
C_L	roll moment coefficient
C_M	pitch moment coefficient
C_T	thrust coefficient
e_{pc}	root cut-out divided by R
k	reduced frequency based on free-stream velocity, ω/v
K_m	normalized apparent mass
K_I	normalized rotary inertia
L	gain of Hohenemser inflow law
[L]	matrix of inflow gains
$[\mathcal{L}]$	[L] normalized on V
[L(k)]	complex [L] matrix
[M]	apparent mass matrix
p	flapping frequency, per revolution
r	distance from rotor center, m
R	blade tip radius, m
t	time, sec
[T]	transform for tip loss
J	inflow mass-flow parameter, $\dfrac{(\lambda+\bar{v}_o)(\lambda+2\bar{v}_o)+\mu^2}{\sqrt{(\lambda+\bar{v}_o)^2+\mu^2}}$
V_T	total velocity at rotor, $\sqrt{(\lambda+\bar{v}_o)^2+\mu^2}$
α	disk angle at rotor, $\tan^{-1}\left(\dfrac{\lambda+v_o}{\mu}\right)$
α_s, α_c	hub angles, advancing blade down, nose up, rad
β	flapping angle, rad
γ	Lock number
$\theta_o, \theta_s, \theta_c$	collective and cyclic pitch, rad
λ	normalized free-stream velocity perpendicular to rotor disk
μ	normalized free-stream velocity in the plane of rotor disk
v	induced flow perturbation, $v = v_o + v_s \sin\psi + v_c \cos\psi$
$\bar{v}_o$	steady part of induced flow
v_o, v_s, v_c	induced flow perturbation harmonics
σ	blade solidity
τ	time constant, Hohenemser inflow law
$[\tau]$	matrix of time constants

ψ	blade azimuth angle, rad
ω	frequency of oscillations, per revolution
Ω	rotor speed, rad/sec (RPM in Ref. 20)
$(\dot{\ })$	$d(\ )/dt$
$(\overset{*}{\ })$	$d(\ )/d\psi$

Introduction

From its inception over 30 years ago to its full development today, the theory of dynamic inflow has been driven constantly by the impetus of experimental data. In 1950, Ken Amer noticed that the theoretical pitch-roll damping of helicopters did not agree with flight measurements, Reference 1.

Although most of the differences could be attributed to the angle between thrust and tip-path plane, there remained a discrepancy that Amer attributed to a variation in inflow over the rotor disk. Sissingh provided a mathematical model to explain this phenomenon, Reference 2, and his model initiated the study of dynamic (or variable) inflow. In short, Sissingh showed that the side-to-side thrust perturbation (created by a roll rate) could create perturbations in the induced flow field that substantially affected roll damping. It was essentially this inflow model that was later simplified and extended by Curtiss and Shupe and applied extensively to problems of flight dynamics via an "equivalent Lock number" to account for induced flow perturbations, References 3 and 4.

In 1971-1972, Lockheed performed some wind tunnel tests that would change the course of the theory of dynamic inflow. These tests, on a 7.5 ft. diameter rotor in NASA's 7×10 ft. wind tunnel, measured 15 static rotor derivatives (C_T, C_L, C_M, with respect to θ_0, θ_s, θ_c, α_s, α_c) as functions of advance ratio from $\mu = 0$ to 1.4, Reference 5. The results revealed major qualitative differences between conventional rotor theory and the experimental data. Most importantly, these differences could not be explained by classical excuses (reversed flow, blade elasticity, dynamic stall, etc.). As a result of this comparison, a variable-inflow theory was included in the equations, based on momentum developments similar to those in References 2-4. The results were very interesting. In hover, the momentum-theory model of dynamic inflow provided beautiful correlation with the data. In forward flight, however, the model was of little use in aiding the correlation. As a result, the authors of Reference 5 formulated other theories in forward flight based on simple vortex considerations. Finally, they formulated an empirical inflow model based on the best fit of the static data.

The above narrative describes the development of the static theory of variable inflow. In 1953, Carpenter and Fridovitch noticed that there was a time delay in the development of induced flow following rapid changes in blade collective pitch, Reference 6. They formulated a time constant for induced flow that was based on the apparent mass of an impermeable disk, and they showed that this time constant accounted for the measured transients in induced flow. In 1972, new experimental data (Reference 7) spurred the incorporation of these time delays into the variable inflow theories, Reference 8. Reference 8 compares theory and experiment for the oscillatory response (magnitude and phase) of roll and pitch moments due to oscillations of θ_0, θ_s, θ_c, α_s, and α_c. These results show that the variable inflow theories of Reference 5, while giving good static correlation, give poor correlation as ω is increased. Furthermore, the data show that the cause of the poor correlation is that the effect of variable inflow decreases with increasing ω. In other words, the induced flow does not have time to respond to rapid changes in loads, which points back to the need for time delays such as those in Reference 6. As a result of this new information, the apparent mass terms were incorporated into both the empirical and momentum-theory variable inflow models; and thus was created dynamic inflow theory, Reference 8.

Background

Before going on to the further developments in dynamic inflow, it might be good first to review the form of the dynamic inflow theories. First, dynamic inflow assumes a limited number of induced flow distributions of unspecified magnitude. The relative amounts of each distribution (that might be present at a particular instant in time) become degrees of freedom in the dynamic analysis. Although several alternatives have been tried through the years, it is now believed that the most useful is

$$v(r,\psi) = v_0 + v_s \frac{r}{R} \sin\psi + v_c \frac{r}{R} \cos\psi$$

$$(1)$$

Some investigators have used only the v_s and v_c terms, References 9-10; and some have added second-harmonic terms, References 11-12. However, in forward flight for rotors with 3 or more blades, the model in Eq. (1) has proved to be the most useful.

In dynamic inflow theory, the air mass degrees of freedom (v_0, v_s, v_c) are described by differential equations as follows.

$$[\tau]\begin{Bmatrix} \overset{*}{\nu_o} \\ \nu_s \\ \nu_c \end{Bmatrix} + \begin{Bmatrix} \nu_o \\ \nu_s \\ \nu_c \end{Bmatrix} = [L]\begin{Bmatrix} C_T \\ C_L \\ C_M \end{Bmatrix}_{aero} \qquad (2a)$$

or

$$[M]\begin{Bmatrix} \overset{*}{\nu_o} \\ \nu_s \\ \nu_c \end{Bmatrix} + [L]^{-1}\begin{Bmatrix} \nu_o \\ \nu_s \\ \nu_c \end{Bmatrix} = \begin{Bmatrix} C_T \\ C_L \\ C_M \end{Bmatrix}_{aero} \qquad (2b)$$

Several explanations are in order for Eq. (2). First, the quantities in Eq. (2) are perturbation values (ν_o, ν_s, ν_c, C_T, C_L, C_M). Thus, the theory is formulated for a linearized analysis. Second, the thrust, roll, and pitch coefficients refer to the aerodynamic components only. Thus, they may be obtained from integrated air loads; or they may be obtained by correction of total hub loads for inertial effects. The matrix [L] is the static coupling matrix between induced flow and aerodynamic loads. The matrix [M] represents the apparent inertia of the air mass, and $[\tau] = [L][M]$ is a matrix of time constants.

Several different definitions of [L] have been used throughout the years. For example, some have used $< C_T -C_L -C_M >$ on the right-hand side since this avoids negative apparent mass elements. Also, some have factored out of [L] the mass flow parameter, V,

$$[L] = \frac{1}{V}[\mathcal{L}] \qquad (3)$$

in order to make [$\mathcal{L}$] a function of disk angle only and not of free-stream velocity. In addition Reference 13 outlines a nonlinear version of Eq. (2) in which ν_o, ν_s, ν_c, C_T, C_L, C_M are total quantities rather than perturbation quantities. This is accomplished with the replacement of V by V_T in the C_T terms,

$$[L] = [\mathcal{L}]\begin{bmatrix} V_T & 0 & 0 \\ 0 & V & 0 \\ 0 & 0 & V \end{bmatrix}^{-1} \qquad (4)$$

where V_T is the normalized flow at the rotor and V is a weighted downstream velocity.

$$V_T = \sqrt{\mu^2 + (\lambda+\bar{\nu}_o)^2}, \quad V = \frac{d}{d\bar{\nu}_o}(\bar{\nu}_o V_T) \qquad (5a,b)$$

The detailed formulation of the elements [$\mathcal{L}$] and [M] is the essence of the theory of dynamic inflow. All investigators, however, have chosen [M] to be a diagonal matrix of the form

$$[M] = \begin{bmatrix} K_m & 0 & 0 \\ 0 & -K_I & 0 \\ 0 & 0 & -K_I \end{bmatrix} \qquad (6)$$

where K_m and K_I are the nondimensional mass and moment of inertia of the participating air mass. Thus far, no one has considered the explicit effect of tip loss on the [$\mathcal{L}$] and [M] matrices. A theoretical case can be made for replacing K_m by $B^3 K_m$, K_I by $B^5 K_I$, and for transforming [$\mathcal{L}$] to $T^T \mathcal{L} T$ where

$$[T] = \begin{bmatrix} B & 0 & 0 \\ 0 & B^2 & 0 \\ 0 & 0 & B^2 \end{bmatrix} \qquad (7)$$

The transformation in Eq. (7) assumes that only the radius BR is effective in dynamic inflow, but this has not been verified experimentally. Thus, we continue to use [M] and [L] uncorrected for tip loss.

Correlation with Flapping Data

With the form of dynamic inflow theory now set forth, we can proceed to outline the development of the [L] and [M] matrices and of the V parameter. In Reference 8, presented at this same conference 10 years ago, the experimental data from Reference 7 are compared with results calculated from new dynamic inflow theory (including both [$\mathcal{L}$] and [M]). In hover, [$\mathcal{L}$] and [M] are taken from momentum theory and are diagonal matrices.

$$\mathcal{L}_{11} = \frac{1}{2}, \quad \mathcal{L}_{22} = \mathcal{L}_{33} = -2. \quad V = 2\bar{\nu}_o$$

$$M_{11} = \frac{8}{3\pi}, \quad M_{22} = M_{33} = \frac{-16}{45\pi} \qquad (8a-e)$$

The results are extremely interesting. Fig. 1 gives the magnitude and phase of both roll and pitch moments in hover due to oscillations in θ_s. The frequency is given per revolution. The theory without dynamic inflow is not even qualitatively accurate. When quasi-steady inflow is included (no apparent mass) the data are precisely captured for $\omega < .2$. For larger ω, the quasi-steady theory is inaccurate; but the unsteady theory (with apparent mass) captures the effect. Fig. 2 presents a similar plot from Reference 8 but for oscillations of shaft angle. Because of the theoretical symmetry in roll and pitch oscillations, data for both excitations are presented together. Above $\omega = .3$, the two sets of data diverge due to stand resonances. For $\omega < .3$ both agree. Once again, we find that the theory with no dynamic inflow is qualitatively in error but that momentum theory completely captures the response for $\omega < .3$. It is hard to look at Figs. 1 and 2 and not be impressed that dynamic

189

inflow is not only a true physical occurrence but that it is also well-modeled in hover by momentum theory with apparent-mass time delays.

At the same time as Army scientists were discovering that dynamic inflow was necessary to correlate the Lockheed data, an Army contractor at Washington University made the identical discovery in an entirely different test, Reference 14. Fig. 3 presents the data of Hohenemser and Crews for pitch stirring excitation. Rather than momentum theory, they used parameter identification to determine a gain L and a time constant τ for an inflow theory. Amazingly, the values of L and τ they obtained turned out to be within a few percent of the similar values from momentum theory; and the correlation with data was excellent. This is further verification of the validity and universality of dynamic inflow. It should be noted that the researchers in Reference 14 (along with D. Banerjee) also attempted to identify a full [L] matrix from transient blade dynamics. However, because their rotor could not be excited in collective pitch, they were unable to develop an adequate response to identify [L].

The good news from the experiments in References 7 and 14 was that momentum theory is nearly perfect in hover. The bad news was that it is nearly useless in forward flight. To be more specific, experimental data in forward flight also showed large deviations from conventional theory, but momentum theory could not make up the difference. There was one bright spot, however. The empirical model, which had been identified based on static ($\omega=0$) derivatives, gave very good agreement with dynamic data for all ω provided that the apparent mass terms were added. This implies that the same apparent mass terms are valid at all advance ratios and that the empirical model is not far from accurate. There are, however, several major problems with the empirical model. First, it is inconveniently formulated in terms of tabulated coefficients. Second, it has no fundamental basis in aerodynamics. Third, the [L] matrix shows singularities at μ = .32 and μ = .80. Fourth, and the most serious, the empirical model is formulated only for edgewise flow. Therefore, there is no accounting for the transition from hover to forward flight.

In summary, the aforementioned experimental data clearly show that, although momentum theory is adequate in hover, a different theory is required for forward flight. Other experimental data and theories were also developed during this time, e.g. Reference 15, but none provided an adequate theory for forward flight.

Pitt Model

The first serious attempt to develop a forward-flight dynamic inflow theory is found in Reference 16. Here, Ormiston began to sort out the various induced-flow components of an actuator disk. The effort fell short due to the complexities of blade motion that are coupled into the lift-flow problem. It became clear that one would have to isolate the induced flow from the blade dynamics in order to solve the problem. This was soon done; and, in 1981, Pitt and Peters introduced a new formulation of dynamic inflow, based on fundamental principles and a rigorous actuator-disk theory, Reference 11.

This theory provides a smooth transition from hover to edgewise flow and has no singularities. In hover, it is identical to classical momentum theory (both for [M] and [L]); and, in forward flight, it develops similar characteristics to those of the empirical model. In the absence of direct experimental inflow measurements, the model has been compared to numerical wake computations, Reference 17. For the static case, comparisons are made with the Landgrebe prescribed wake model applied to a 4-bladed lifting rotor, Reference 18. Figs. 4-6 show this comparison for the nine inflow derivatives, L_{ij}, as functions of disk angle of attack (0° = edgewise flow, 90° = hover). Results from Landgrebe's computer program are labelled "WAKE" on the figures. Clearly, the Pitt model gives reasonable results at all disk angles.

For the dynamic case, the Pitt model has been compared with a Theodorsen-type actuator-disk theory for frequency-response calculations, Fig. 7. In the results of the Pitt model, labelled "superposition of pressures", the formulation assumes that the harmonic induced velocities are all in phase. Consequently, these velocities create pressures that add as in Eq. (2b): 1) in-phase loads due to L, and 2) out-of-phase loads due to M. In the other results, labelled "superposition of velocities", the formulation assumes that the oscillatory loads are all in phase. The resultant induced velocities are then calculated by an involved, Theodorsen-type integration over the entire wake, Reference 17. One must assume that true rotor behavior would be some mixture of the two results. Therefore, the agreement between the two results is confirmation that the simple formulation of Eq. (2b) is adequate. Thus, Figs. 4-7 attest to the reasonableness of the actuator-disk model even for modeling a 4-bladed rotor with flapping dynamics and wake contraction.

The exact formulation of the Pitt model is given below.

$$[L] = \frac{1}{V}\begin{bmatrix} \dfrac{1}{2} & 0 & \dfrac{15\pi}{64}\sqrt{\dfrac{1-\sin\alpha}{1+\sin\alpha}} \\[3mm] 0 & \dfrac{-4}{1+\sin\alpha} & 0 \\[3mm] \dfrac{15\pi}{64}\sqrt{\dfrac{1-\sin\alpha}{1+\sin\alpha}} & 0 & \dfrac{-4\sin\alpha}{1+\sin\alpha} \end{bmatrix}$$

$$(9a)$$

$$[M] = \begin{bmatrix} \dfrac{128}{75\pi} & 0 & 0 \\[3mm] 0 & \dfrac{-16}{45\pi} & 0 \\[3mm] 0 & 0 & \dfrac{-16}{45\pi} \end{bmatrix}$$

$$(9b)$$

Several comments are in order. First, α is the wake angle at the rotor

$$\alpha = \tan^{-1}\left(\frac{\lambda+\bar{v}_o}{\mu}\right) \qquad (10a)$$

Therefore, $\alpha = 0°$ corresponds to edgewise flow and $\alpha = 90°$ to hover or axial flight. Second, the V parameter from Eq. (5b) is taken from momentum theory.

$$V = \frac{(\lambda+\bar{v}_o)(\lambda+2\bar{v}_o)+\mu^2}{\sqrt{(\lambda+\bar{v}_o)^2+\mu^2}} \qquad (10b)$$

Thus, in edgewise flow $V = \mu$ and in axial flow $V = \lambda + 2\bar{v}_o$. Because of this, the [L] matrix in Eq. (8a) exactly reduces to momentum theory at $\alpha = 90°$. The elements for $\alpha = 90°$ are consequently identical to virtually all of the previous work in dynamic inflow, References 2, 3, 4, 5, 8, and 9. [It should be noted, however, that Eq. (9a) for $\alpha = 90°$ differs significantly from the corresponding matrix in References 19 and 20. In particular, there is a difference of the factor of 2 on the L_{22} and L_{33} terms. A detailed discussion of this difference is given in Reference 13.] It follows that the Pitt model provides the identical good correlation in hover as does momentum theory.

Another interesting aspect of Eq. (9a) is the (3,1) element. This element provides for a fore-to-aft gradient in induced flow due to thrust and is identical to the Coleman equation for the classical Glauert constant, Reference 21. This L_{31} term is also one of the more important terms found from the empirical model. The other elements of L behave similarly to the empirical model. Of special importance is the fact that $L_{33} = 0$ (at $\alpha=0$) for both models.

With respect to the [M] matrix, the elements in Eq. (6) are also derived from the unsteady, actuator-disk theory. When a uniform lift distribution is used for C_T, the elements are identical to those of momentum theory. When the lift is forced to be zero at the rotor center, however, then M_{11} becomes $\frac{128}{75\pi}$ (= .54) rather than $\frac{8}{3\pi}$ (= .85); while M_{22} and M_{33} remain identical to the values from momentum theory (i.e., from an impermeable disk).

Thus, the Pitt model provides all of the important ingredients for a good dynamic inflow model:

1) Simplicity of closed-form expressions
2) Recovery of momentum theory in axial flow
3) Reasonable behavior for edgewise flow
4) Correlation with wake calculations.

The only missing ingredient from the Pitt model is a direct comparison with experimental flapping data, and that will be given in 'his paper.

Experimental Data for Rotor-Body Motion

In the previous sections, we have described the role of experimental data in the development of dynamic inflow. All of this data has been associated with purely flapping degrees of freedom and with loads normal to the blade disk (β, C_T, C_L, C_M) which relate directly to the normal flow of induced velocities. However, early on in the development of dynamic inflow, investigators realized that dynamic inflow could have an indirect effect on rotor body and inplane motions, thereby influencing lead-lag damping and helicopter pitch-roll dynamics, Reference 22. Here, again, the experimental data played a key role.

Reference 23 describes detailed frequency and damping measurements for a model rotor with inplane and body degrees of freedom. This data did nct agree with theory and motivated the work in Reference 24 which shows that dynamic inflow can explain many of the phenomena found in Reference 23. It was Wayne Johnson, however, Reference 20, who provided the first direct correlation with this more sophisticated data. Reference 20 includes 12 figures, and almost every one of them shows a strong effect of dynamic inflow. For the sake of completeness, we would like to reproduce two of those results here. First, Fig. 8 gives a comparison of measured and calculated frequencies as a function of Ω. In particular, we note a theoretical frequency branch in Fig. 8a labeled λ, which implies that it is dominated by dynamic inflow, although it is certainly coupled with regressing

flapping (β_R) and body pitch (θ). The experimental data agree very well with this branch for $\Omega > 400$ RPM. In comparison, the theory with no dynamic inflow, Fig. 8b, does not have such a branch; and it cannot, therefore, even begin to match the data.

The second result from Reference 20 is given in Fig. 9 and is a comparison of experimental roll damping with results of the Ames analysis (both with and without dynamic inflow). The results show that dynamic inflow gives a substantial improvement in correlation. Also shown in the figure is a similar analysis by Bell Helicopter (with and without dynamic inflow) which was presented at the ITR workshop, Reference 25. One can see that both the Ames and Bell results show the same improved correlation due to dynamic inflow. In general, the ITR results (which included many such comparisons) show that dynamic inflow often has a large effect on rotor-body and inplane damping and that modeling it generally improves correlation. On the other hand, the ITR results also show that, for some modes and frequencies, dynamic inflow has very little effect. Furthermore, there remain discrepancies between theory and experiment that cannot be accounted for by dynamic inflow. Therefore, the major conclusions from such comparisons are: 1) Dynamic inflow can have a pronounced effect on lead-lag and rotor-body damping, and 2) Rotor-body data cannot be used to validate or invalidate a particular dynamic inflow model. The justification for the second conclusion is straightforward. Our predictive capabilities in rotor-body dynamics are not sufficiently refined to isolate the effect of one single phenomenon. On the other hand, our predictive capabilities in flapping response are much better. Therefore, once we identify dynamic inflow as a true physical phenomenon based on flapping response, we have no choice but to: 1) believe that it has an effect on inplane and body dynamics, as shown in Reference 25, and 2) to include it in such analyses.

Comparison of Pitt Model with Static Data

The previous sections of this paper have dealt with the history of dynamic inflow. In particular, we have:

1) Reviewed the development of dynamic inflow theory and its close ties to experimental data;
2) Described the most promising inflow model, the Pitt model;
3) Shown that, although dynamic inflow is often important for inplane dynamics and rotor-body problems, only pure blade flapping response provides an appropriate data base to verify a particular inflow model.

With this as background, we are ready to introduce some new results in this paper.

In these results, we compare the Pitt model to the Lockheed-Ames data of Reference 7. The first comparison concentrates on the nine static derivatives analyzed in Reference 5. The derivatives are for $p = 1.17$ and are given as functions of advance ratio for $0 < \mu < .5$. Comparison is made of the theory without dynamic inflow, momentum theory, the Pitt model, and the experimental data. All coefficients are normalized on σa.

We begin with the C_T derivatives, Figs. 10a-c. For C_T/θ_O, momentum theory and the Pitt model give equally good data correlation. For C_T/θ_S, the data show an initial sign reversal followed by a return to a more conventional response. The Pitt model also gives this sign reversal, which is not predicted by momentum theory. For $\mu > .2$, however, momentum theory is a little better. For C_T/θ_C, only the Pitt model gives any derivative, but no data is available for comparison. We now turn to the C_L derivatives, Figs. 10d-f. For C_L/θ_O, momentum theory is little different from the no-inflow theory; and neither gives even a qualitative correlation. The Pitt model, however, is nearly perfect here. For C_L/θ_S, momentum theory is again completely inadequate while the Pitt model is very good. In C_L/θ_C, both inflow models do fairly well for $\mu < .4$. The theory without dynamic inflow is not satisfactory. Next, we consider the C_M derivatives, Figs. 10g-i. For C_M/θ_O, only the Pitt model predicts the large increase in the derivative for $\mu < .2$; but momentum theory does better at higher μ. For C_M/θ_S, momentum theory is slightly better than the Pitt model; and, for C_M/θ_C, the Pitt model correctly predicts the increase in derivative for $\mu > .1$. For $\mu > .1$, however, momentum theory seems better.

The above static comparisons have a mixture of judgements with momentum theory sometimes better and with the Pitt model sometimes better. To obtain a quantitative measure of the relative merits of the models we define the following scoring system for correlation of experiments with theoretical results.

0 - no better than "no dynamic inflow"
1 - moves theory in correct qualitative direction
2 - substantially improves data correlation
3 - excellent correlation with data

The first two columns of Table 1 give a comparison of methods under this scoring system. Numbers given are average scores over the above 8 static derivatives. The empirical model, not shown in Figs. 10a-i, is included based on the results in Reference 5.

Table 1. Comparison of methods.

Model Data	Static Data $p = 1.17$	Dynamic Data $p = 1.15$
Momentum Theory	1.6	0.8
Pitt Model	2.5	2.1
Empirical Model	2.7	2.2

The Pitt model is an overall winner over momentum theory, the former averaging between "substantial improvement" and "excellent correlation" while the latter averages a whole category less. Surprisingly, the Pitt model is almost as good as the Empirical model which was identified solely on the basis of best fit of this static data. In the following section, we will be able to compare at a different value of flapping frequency, $p = 1.15$.

Comparison with Dynamic Data

We are now ready to compare the Pitt model with the dynamic measurements of Reference 7. It is interesting that the original attempt at correlation of this data was presented at the First Decennial Dynamics Specialists' Meeting, ten years ago. This data, for $p = 1.15$, is nearly the same configuration as that of the static data. Thus, the $\omega = 0$ results closely resemble the static data of Fig. 10. The original dynamic data in Reference 8 was presented only for $\mu = .51$. Here, we expand the data base to include three advance ratios: $\mu = .27$, .36, .51. Thus, we present entirely new data correlations and provide a broader and fairer comparison. Only roll and pitch moments are given because no dynamic thrust measurements were made. Consequently, the following figures are for the 6 dynamic roll and pitch moment derivatives (magnitude and phase). For the sake of brevity, phase angles are not presented for all derivatives. However, the phase angles that are given are entirely representative of those omitted.

Figs. 11-13 give $C_L/\sigma a$ due to θ_o at three advance ratios. The points near $\omega = 0$ correspond to the static data in Fig. 10. We give the magnitude of the response as a function of ω. Phase is given only for $\mu = .36$ (our reference advance ratio) but is typical of the other advance ratios. Several items are noteworthy. First, the static results at $p = 1.15$ (inferred from $\omega = 0$) show the same deviations as do the derivatives in Fig. 10d. In particular, the derivative from the Pitt model is smaller than the data, and the null point is shifted. Despite this, however, the theory does a good job of data correlation as ω is

increased. For example, at all 3 values of μ, the no-inflow and momentum theories show a nearly null point at $\omega = .4$ accompanied by a near discontinuity in phase from 90° to 270°. The data and the Pitt model, however, do not follow this pattern and show a level amplitude and smooth phase change through the region. (Recall that $\theta = 0°$ and $\theta = 360°$ are identical.) Another note here is that momentum theory provides virtually no improvement in theory, whereas the Pitt model provides a positive influence.

In Figs. 14-16, we examine $\partial C_L/\partial \theta_s$ at the same three advance ratios. The phase at $\mu = .36$ is representative. Unlike $\partial C_L/\partial \theta_o$, this derivative is nonzero in hover (Fig. 1) so that we truly have four advance ratios to compare. In hover, momentum theory and the Pitt model are identically good. As advance ratio increases, however, the data begin to change dramatically while the no-inflow and momentum theories barely budge. The Pitt model on the other hand changes with the data and provides nearly identical static correlation ($\omega = 0$). Similarly, as ω increases, the Pitt model causes the theory to follow the data well up to $\omega = .6$. Beyond that, the data seem to fall below all three theories. In terms of phase, the Pitt model does well except for the rapid change in phase at $\omega = .4$ associated with the antiresonance. Thus, the Pitt model does well at all advance ratios from 0 to .51. For the remainder of the derivatives, we will present only the $\mu = .36$ correlations since these are fairly representative.

Fig. 17 gives $\partial C_L/\partial \theta_c$. For comparison purposes we can again refer to Fig. 1 since, in hover, C_L/θ_c is analogous to $\partial C_M/\partial \theta_s$. At $\mu = 0$, the momentum theory and Pitt model are equally good (being identical); and they show the large drop in static derivative followed by a peak and return to no-inflow values. At $\mu = .36$, both theories still show the proper reduction in static value, but the Pitt model does better at reproducing the return to no-inflow theory. Both theories do well on phase angle (not shown).

We now turn to pitch-moment data. Fig. 18 provides $C_M/\sigma a$ with θ_o. This derivative is zero in hover but is quite large at $\mu = .36$. In this case, momentum theory shows too much reduction in the static value while the Pitt model is nearly perfect. (Recall that the momentum theory was better at $p = 1.17$.) One notices two ripples in the data (at $\omega = .4$ and $\omega = .7$). These are stand resonances and introduce some contamination of the data. It is possible that these resonances account for some deviations in roll-moment data, especially the null point in $\partial C_L/\partial \theta_s$. The phase angle for $\partial C_M/\partial \theta_c$ (not shown) is insensitive to inflow model, and all models show equally good correlation.

In Fig. 19, we have $\partial C_M/\partial \theta_s$ at $\mu = .36$, which can be compared with the hover value in Fig. 1. The stand resonance is clearly seen at $\omega = .4$ as an anamolous data point. Both the Pitt model and the momentum theory do well at $\mu = .36$ with the slight edge going to momentum theory. C_M with θ_s is the only derivative for which momentum theory is consistently better than the empirical and the Pitt models. Once again, all models give good phase correlation.

The final figure to be presented is $C_M/\sigma a$ with θ_c, Fig. 20. Both magnitude and phase are shown, and the corresponding hover results are $\partial C_L/\partial \theta_s$, Fig. 1. The Pitt model predicts the increased static derivative ($\omega = 0$), and the model does well for $\omega < .5$. For larger values of ω, it is hard to distinguish the best theory. On phase angle, the Pitt model gives the correct trend at all ω's but does not capture the complete phase shift near $\omega = .4$. Once again, the stand resonance could be a factor.

We can again use the scoring method mentioned earlier in the paper to compare the various models. All advance ratios and derivatives are included in the scoring, and we also rank the empirical model of Reference 8 (although empirical results are not plotted here). The scoring is given in the last column of Table 1. The usefulness of momentum theory diminishes greatly as compared with the static case. It produces a score of less than unity. (Most of the time it does not even move the theory in the right direction.) The Pitt model, on the other hand, scores close to the empirical model; and both give, on the average, more than a substantial improvement in correlation. The overall impression of Table 1 places the Pitt model as the best model in forward flight.

Conclusions

Over the past thirty years, the theory of dynamic inflow has developed due to the desire to correlate with experimental data. The preponderance of data correlations over that time (as well as the new comparisons presented here) lead to the following conclusions:

1) The effect of dynamic inflow has been demonstrated to be a valid physical phenomenon that can change the qualitative nature of rotor response in hover and forward flight.
2) In hover, dynamic inflow is represented nearly exactly by momentum theory coupled with apparent mass terms (three first-order equations).
3) In forward flight, momentum theory does very poorly and cannot capture the major effects of dynamic inflow.
4) The Pitt model, developed from an analytical base, provides excellent data correlation in forward flight and is

identical to momentum theory in hover. Thus, it stands as the premier model for rotor analysis.
5) Although dynamic inflow is often important for problems of inplane and rotor-body dynamics (and often improves correlation), such studies are not reliable for the validation of inflow models. Dynamic inflow theories must be verified on the basis of flapping response and inflow measurements.

Acknowledgement

References

1. Amer, K. B., "Theory of Helicopter Damping in Pitch or Roll and a Comparison with Flight Measurements," NACA TN-2136, October 1950, p. 11.

2. Sissingh, G. J., "The Effect of Induced Velocity Variation on Helicopter Rotor Damping in Pitch or Roll," Aeronautical Research Council Paper No. 101, Technical Note No. Aero 2132, November 1952.

3. Shupe, N. K., A Study of the Dynamic Motions of Hingeless Rotored Helicopters, Ph.D. Thesis, Princeton, September 1970.

4. Curtiss, H. C., Jr. and Shupe, N. K., "A Stability and Control Theory for Hingeless Rotors," Proceedings of the 27th Annual National Forum of the American Helicopter Society, May 1971, Paper No. 541.

5. Ormiston, Robert A. and Peters, David A., "Hingeless Rotor Response with Nonuniform Inflow and Elastic Blade Bending," Journal of Aircraft, Vol. 9, No. 10, October 1972, pp. 730-736.

6. Carpenter, P. J. and Fridovitch, B., "Effect of Rapid Blade Pitch Increase on the Thrust and Induced Velocity Response of a Full Scale Helicopter Rotor," NACA TN-3044, November 1953.

7. Kuczynski, W. A. and Sissingh, G. J., "Characteristics of Hingeless Rotors with Hub Moment Feedback Controls Including Experimental Rotor Frequency Response," NASA CR 114427, January 1972.

8. Peters, David A., "Hingeless Rotor Frequency Response with Unsteady Inflow," Rotorcraft Dynamics, NASA SP-352, February 1974, pp. 1-13.

9. Ormiston, Robert A., "Application of Simplified Inflow Models to Rotorcraft Dynamic Analysis," _Journal of the American Helicopter Society,_ Vol. 21, No. 3, July 1976, pp. 34-39.

10. Gaonkar, Mitra, and Reddy, "Feasibility of a Rotor Flight Dynamics Model with First-Order Cyclic Inflow and Multi-Blade Modes," Proceedings of the AIAA Dynamics Specialists' Meeting, Atlanta, Georgia, April 9-10, 1981, p. 15.

11. Pitt, Dale M. and Peters, David A., "Theoretical Predicticns of Dynamic Inflow Derivatives," _Vertica,_ Vol. 5, No. 1, March 1981.

12. Gaonkar, et al., "The Use of Actuator-Disc Dynamic Inflow for He'copter Flap-Lag Stability," _Journal of the American Helicopter Society,_ Vol. 28, No. 3, July 1983, pp. 79-88.

13. Peters, David A., "The Importance of Steady and Dynamic Inflow on the Stability of Rotor-Body Systems," Proceedings of the ITR Methodology Workshop, NASA-Ames Research Center, June 21-22, 1983.

14. Crews, S. T., Honenemser, K. H., and Ormiston, R. A., "An Unsteady Wake Model for a Hingeless Rotor," _Journal of Aircraft,_ Vol. 10, No. 12, December 1973, pp. 758-760.

15. Azuma, Akira and Nakamura, Yoshiya, "Pitch Damping of Helicopter Rotor with Nonuniform Inflow," _Journal of Aircraft,_ Vol. 11, No. 10, October 1974, pp. 639-646.

16. Ormiston, Robert A., "An Actuator Disk Theory for Rotor Wake Induced Velocities," AGARD Specialists Meeting on the Aerodynamics of Rotary Wings, Marseille, France, September 13-15, 1972.

17. Pitt, Dale M. and Peters, David A., "Rotor Dynamic-Inflow Derivatives and Time Constants from Various Inflow Models," 9th European Rotorcraft Conference, Stresa, Italy, September 13-15, 1983, Paper No. 55.

18. Landgrebe, A. J., "An Analytical Method for Predicting Rotor Wake Geometry," _Journal of the American Helicopter Society,_ Vol. 14, No. 4, October 1969.

19. Johnson, Wayne, _Helicopter Theory,_ Princeton University Press, 1980, pp. 520-526.

20. Johnson, Wayne, "Influence of Unsteady Aerodynamics on Hingeless Rotor Ground Resonance," _Journal of Aircraft,_ Vol. 19, No. 8, August 1982, pp. 668-673.

21. Coleman, Feingold, and Stempin, "Evaluation of the Induced Velocity Field of an Idealized Helicopter Rotor," NACA WRL-126, June 1945.

22. Peters, David A. and Gaonkar, Gcpal H., "Theoretical Flap-Lag Damping with Various Dynamic Inflow Models," _Journal of the American Helicopter Society,_ Vol. 25, No. 3, July 1980, pp. 29-36.

23. Bousman, W. G., "An Investigation of the Effects of Aeroelastic Couplings on Aeromechanical Stability of a Hingeless Helicopter Rotor," _Journal of the American Helicopter Society,_ Vol. 26, No. 1, January 1981, pp. 46-54.

24. Gaonkar, G. H., Mitra, A. K., Reddy, T.S.R., and Peters, D. A., "Sensitivity of Helicopter Aeromechanical Stability to Dynamic Inflow," _Vertica,_ Vol. 6, No. 1, January 1982, pp. 59-75.

25. Bousman, W. G., "Rotorcraft Stability Methodology Assessment," Proceedings of the ITR Methodology Workshop, NASA-Ames Research Center, June 21-22, 1983.
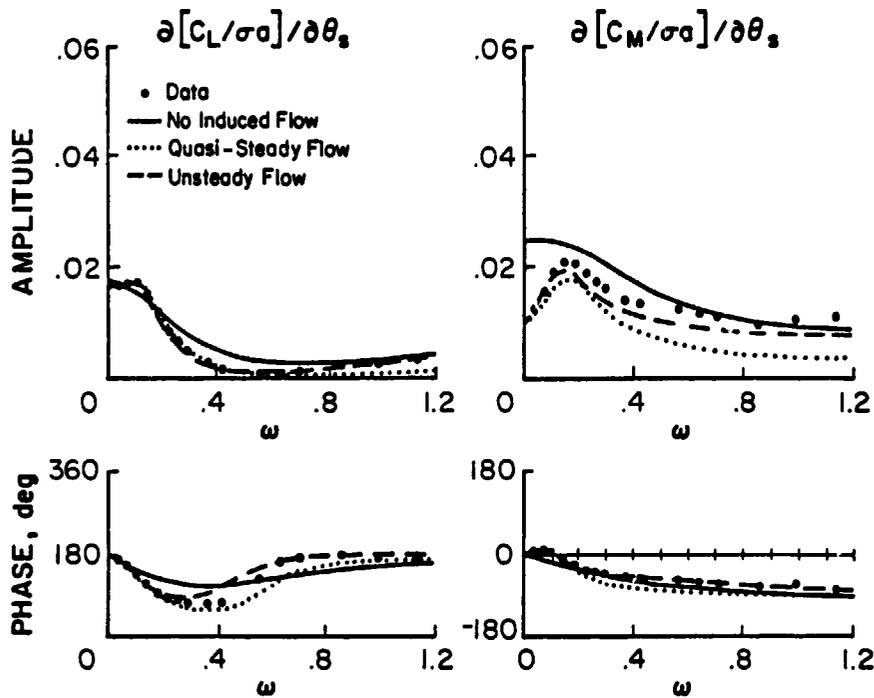
Figure 1. Rotor Response to Cyclic Pitch in Hover, p=1.15, γ' =4.25, B=.97, e_{pc}=.25, μ =0, σa=.7294, $\overline{\nu_0}$ =.03, Θ_0 =4°, λ =0 momentum theory, single rotating mode.
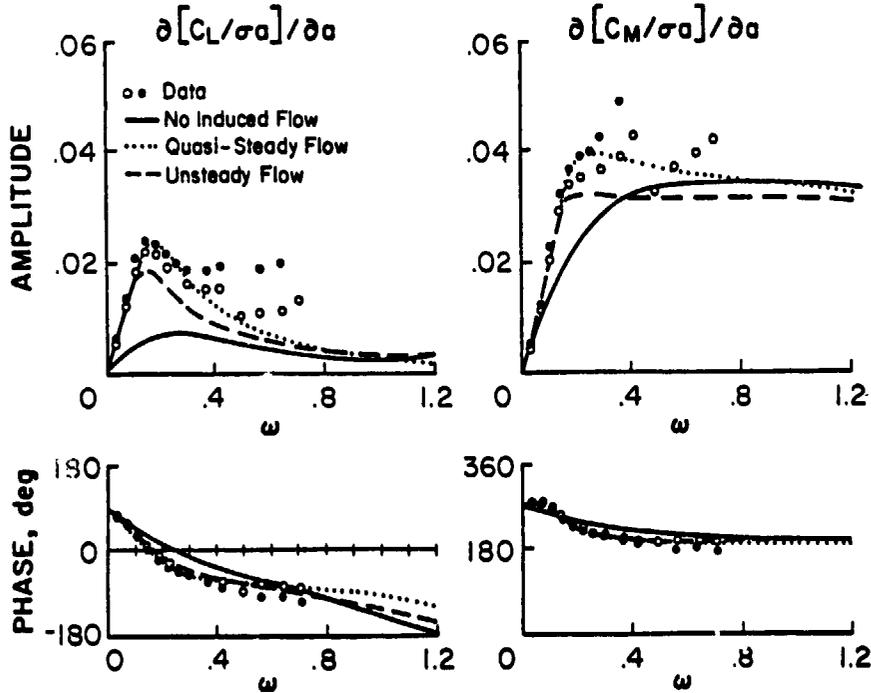
Figure 2. Rotor response to Hub Motions in Hover, p=1.15, γ' =4.25, B=0.97, e_{pc}=0.25, μ =0, σa=.7294, λ=0, $\overline{\nu_0}$ =.03, momentum theory, single rotating mode.
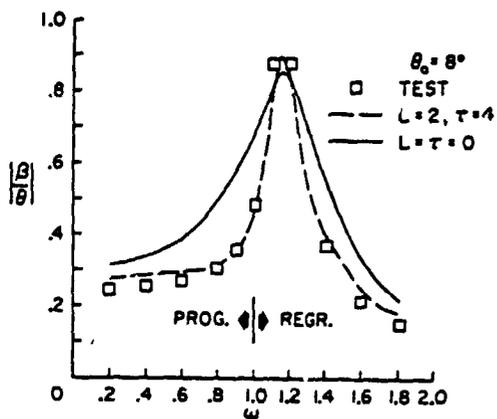
Figure 3. Rotor Response to Pitch Stirring,
p = 1.21, γ = 4.0, μ = 0, β = 0.97.
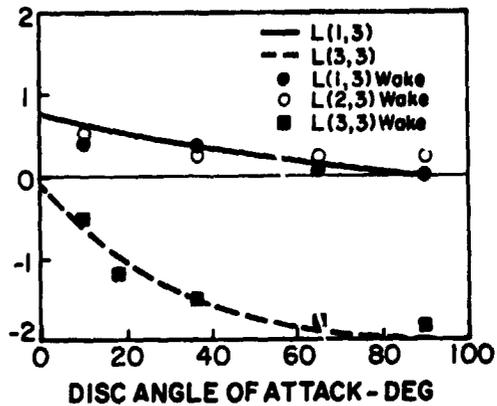
Figure 6. Verification of Third Column of L.
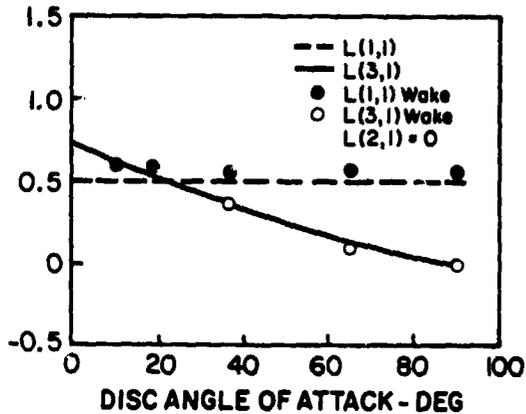
Figure 4. Verification of First Column of L.
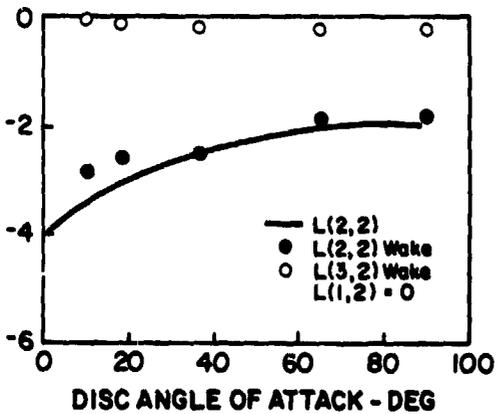
Figure 5. Verification of Second Column of L.
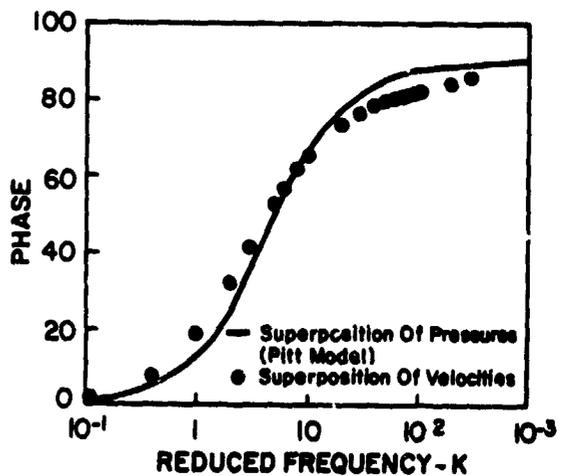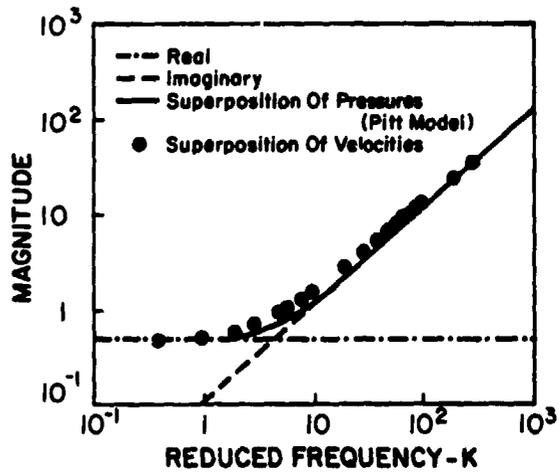
Figure 7. Comparison of Harmonic Pressure
Distributions as Calculated by the Pitt Model
(Superposition of Apparent-Mass Pressure) with
those of an Unsteady Wake Calculation (Super-
position of Velocities).

Figure 9. Comparison of roll mode damping.
a) Bell Helicopter model, b) NASA Ames
model.
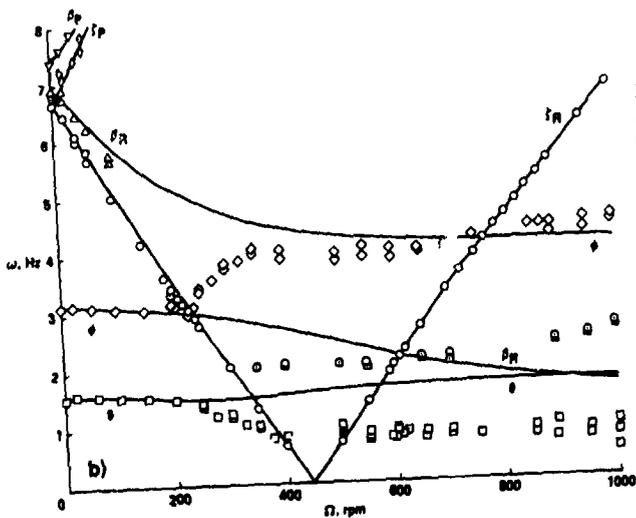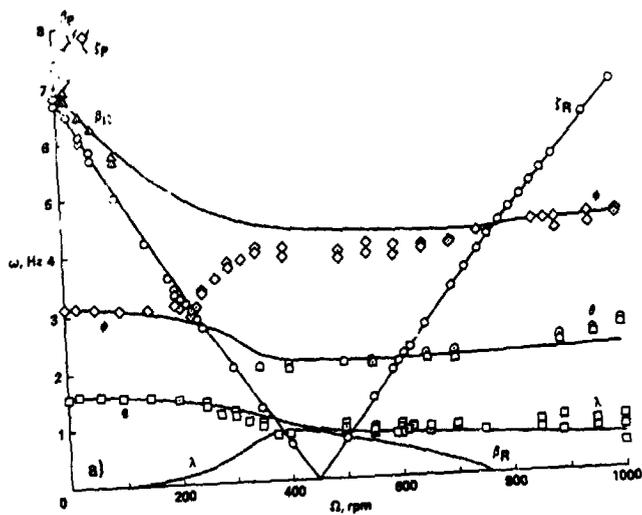
Figure 8. Modal frequencies as a function
of rotor speed for configuration 4 (Refer-
ence 20). Comparison of measurements
(open symbols) and calculation (lines).
a) With inflow dynamics; b) without inflow
dynamics.
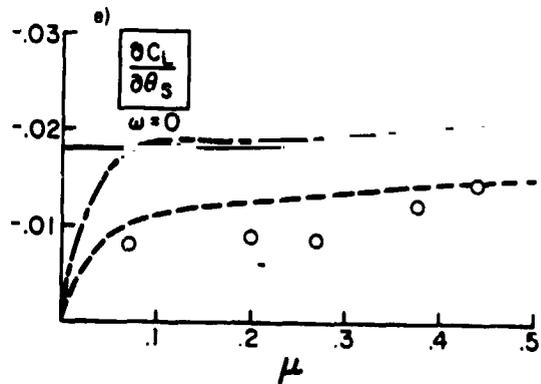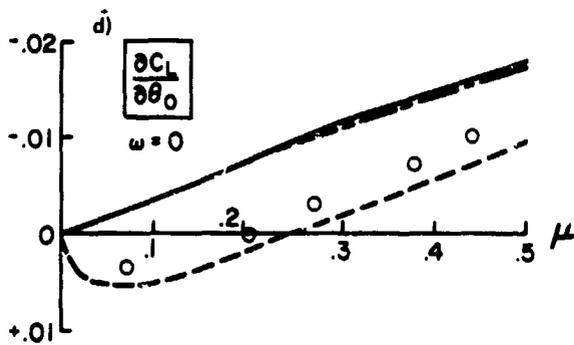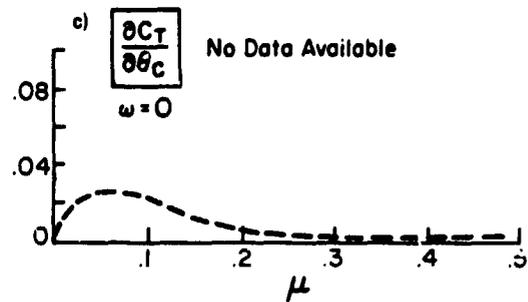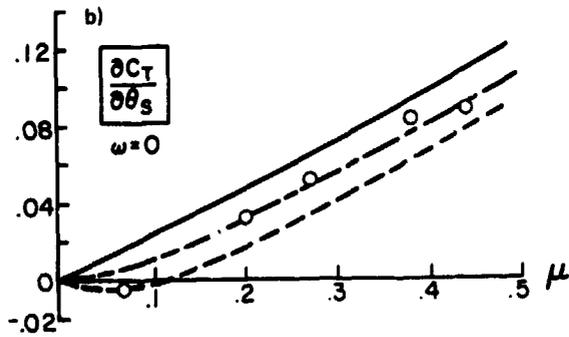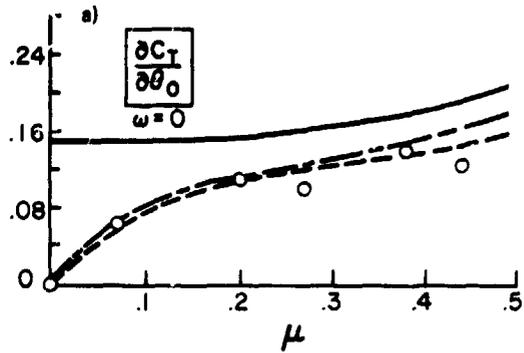
Figure 10. Rotor response for $\omega = 0$, $p = 1.17$, $\gamma = 4.2$, $B = 0.97$, $e_{pc} = 0.25$, $\sigma a = 0.73$, $\bar{\nu}_0 = \lambda = 0$, all coefficients normalized on σa.
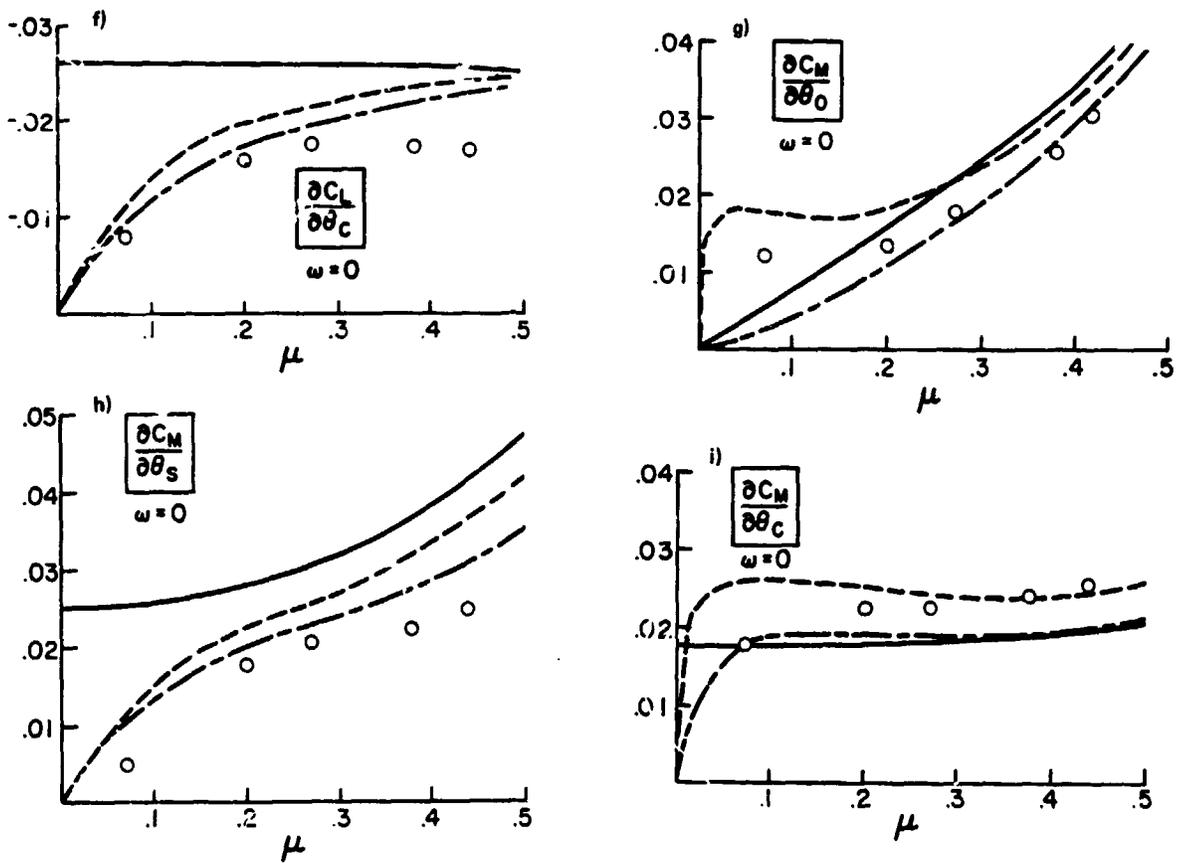
Figure 10. Concluded.
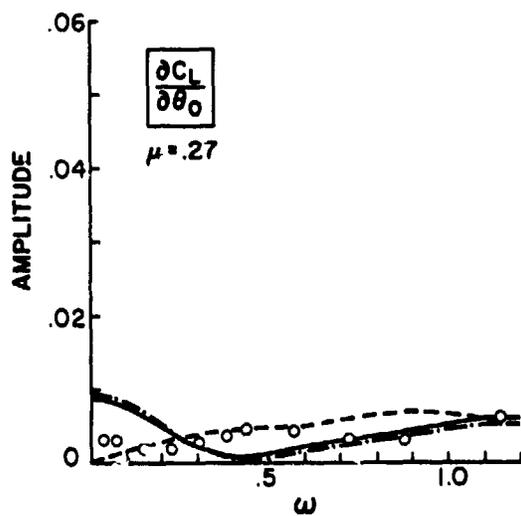
igure 11. Rotor response in forward
flight, $C_L/\sigma a$ due to θ_0 for $\mu = 0.27$,
$\rho = 1.15$, $\gamma = 4.25$, B = 0.97, $e_{pc} = 0.25$,
$\sigma a = 0.73$, $\bar{v}_0 = \lambda = 0$. (See Fig. 10 for
legend.)
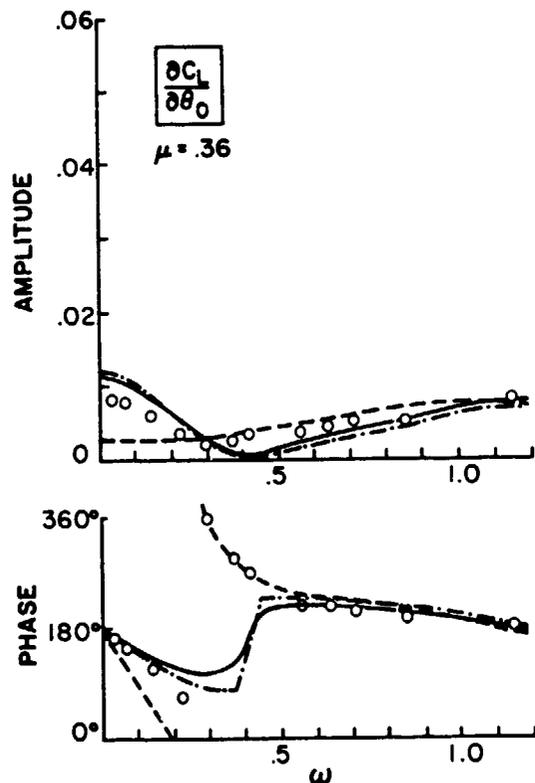
Figure 12. Rotor response in forward flight, $C_L/\sigma a$ due to θ_0 for $\mu = 0.36$, $p = 1.15$, $\gamma = 4.25$, $B = 0.97$, $e_{pc} = 0.25$, $\sigma a = 0.73$, $\bar{\nu}_0 = \lambda = 0$. (See Fig. 10 for legend.)
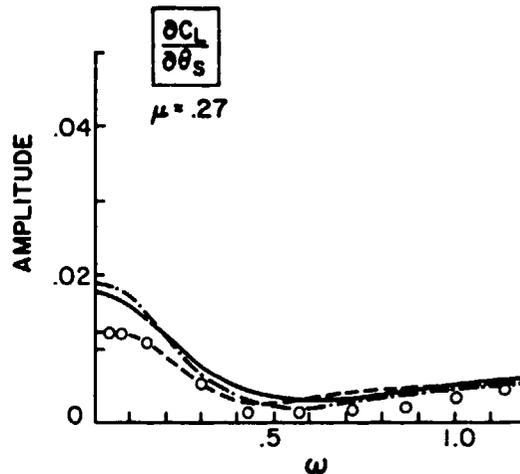
Figure 14. Rotor response in forward flight, $C_L/\sigma a$ due to θ_S for $\mu = 0.27$, $p = 1.15$, $\gamma = 4.25$, $B = 0.97$, $e_{pc} = 0.25$, $\sigma a = 0.73$, $\bar{\nu}_0 = \lambda = 0$. (See Fig. 10 for legend.)

Figure 13. Rotor response in forward flight, $C_L/\sigma a$ due to θ_0 for $\mu = 0.51$, $p = 1.15$, $\gamma = 4.25$, $B = 0.97$, $e_{pc} = 0.25$, $\sigma a = 0.73$, $\bar{\nu}_0 = \lambda = 0$. (See Fig. 10 for legend.)
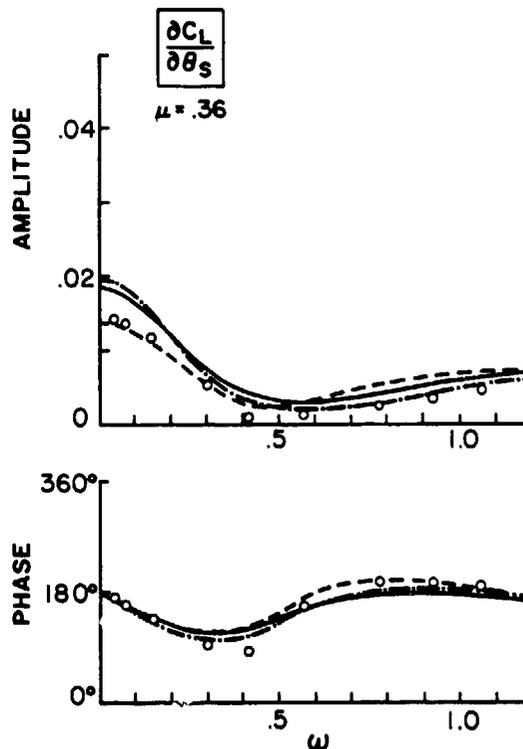
Figure 15. Rotor response in forward flight, $C_L/\sigma a$ due to θ_S for $\mu = 0.36$, $p = 1.15$, $\gamma = 4.25$, $B = 0.97$, $e_{pc} = 0.25$, $\sigma a = 0.73$, $\bar{\nu}_0 = \lambda = 0$. (See Fig. 10 for legend.)

Figure 16. Rotor response in forward flight, $C_L/\sigma a$ due to θ_s for $\mu = 0.51$, $p = 1.15$, $\gamma = 4.25$, $B = 0.97$, $e_{pc} = 0.25$, $\sigma a = 0.73$, $\bar{\nu}_o = \lambda = 0$. (See Fig. 10 for legend.)

Figure 17. Rotor response in forward flight, $C_L/\sigma a$ due to θ_c for $\mu = 0.36$, $p = 1.15$, $\gamma = 4.25$, $B = 0.97$, $e_{pc} = 0.25$, $\sigma a = 0.73$, $\bar{\nu}_o = \lambda = 0$. (See Fig. 10 for legend.)

Figure 18. Rotor response in forward flight, $C_M/\sigma a$ due to θ_o for $\mu = 0.36$, $p = 1.15$, $\gamma = 4.25$, $B = 0.97$, $e_{pc} = 0.25$, $\sigma a = 0.73$, $\bar{\nu}_o = \lambda = 0$. (See Fig. 10 for legend.)

Figure 19. Rotor response in forward flight, $C_M/\sigma a$ due to θ_s for $\mu = 0.36$, $p = 1.15$, $\gamma = 4.25$, $B = 0.97$, $e_{pc} = 0.25$, $\sigma a = 0.73$, $\bar{\nu}_o = \lambda = 0$. (See Fig. 10 for legend.)

Figure 20. Rotor response in forward flight, $C_M/\sigma a$ due to θ_c for $\mu = 0.36$, $p = 1.15$, $\gamma = 4.25$, $B = 0.97$, $e_{pc} = 0.25$, $\sigma a = 0.73$, $\bar{\nu}_o = \lambda = 0$. (See Fig. 10 for legend.)

DISCUSSION
Paper No. 13

A REVIEW OF DYNAMIC INFLOW AND ITS EFFECT ON EXPERIMENTAL CORRELATIONS
Gopal H. Gaonkar
and
David A. Peters

Wayne Johnson, NASA Ames Research Center: In your conclusions you discussed the qualitative ratings you gave for momentum theory and for the Pitt model, but you neglected to mention that the empirical model you rated best of all. Perhaps you would like to comment on that.

Peters: It would be surprising if the momentum theory did better than the empirical model because the empirical model was identified to give the best possible fit of that data that you could with nine elements in an L matrix. All right, so if I got better I think, well, I must have identified wrong. So what it says is [that] that wasn't good enough because it had these singularities in it and it had the other disadvantages. Now the question is with the Pitt model, which comes from basic principles, how close can I get to the old optimum and it's pretty close. I do just about as good as the empirical model so I'm almost to the optimum that I can get. That is, if you try another tweak to the Pitt model and try to make it better you don't have that much more better that you can get because we already have got about as close as we can.

Dev Banerjee, Hughes: I was curious in your comparison between the empirical model and Pitt's model did you identify the singularities that you saw in the empirical results through Dale Pitt's model?

Peters: The Pitt model does not have these singularities. There were basically two in the empirical model. One was at an advance ratio of 0.8 and we sort of think that that was just the dynamic inflow model trying to explain other things. In other words since you are trying to match the data exactly, the L matrix has to do everything, so we sort of feel that somewhere at 0.8 the reverse flow region is getting so large that maybe we're just not doing that well. The other singularity--I don't know why the empirical model has a singularity at μ of 0.32. That is, at the one place L exists, but L inverse doesn't. At 0.32 it is the opposite. L inverse exists but L doesn't. I have no idea why the Pitt model does not show that. It just shows smooth transitions, the determinant is always positive, it never goes through zero, and I don't know if that's just a numerical coincidence or why the empirical model has that singularity in it. I take it back, there may be one possibility. There was a stand resonance that shows up in some of the data that you can see--you couldn't see it in this too well, but some of the others right around a certain frequency range. You wouldn't think that that would be just at one advance ratio where that would show up as a singularity. I don't know.

Bob Ormiston, U.S. Army Aeromechanics Laboratory: An interesting paper Dave and Gopal. My comment just has to do with one of the conclusions about the use of experimental testing to validate the models. I would think in my opinion that the rotor-body flapping dynamic experiments would be excellent for correlating with dynamic inflow. I tend to agree with you when you say that maybe the inplane measurements aren't the best for correlating this type of aerodynamic analysis, but I don't think you need just pure flapping data say, as opposed to coupled flapping and body motion data. The latter is a lot easier to get in an experiment sometimes as we have found out. Maybe I misinterpreted what you said, but I think that two degrees of freedom are okay.

Peters: I partially agree with you. I think that as we get better that will happen. But here is an example: in the next paper you are going to see that if you put a factor of 2 in some of the terms of the L matrix you can get maybe a 15 to 20 percent change in the damping of roll and pitch and maybe get a slightly better correlation. All right? But if you put a factor of 2 into this flapping data you are going to throw that beautiful correlation completely off. So that makes you scratch your head and say, now wait, if I have to do that much to get this much sensitivity in roll and pitch maybe the other is wrong. But someday we should be able to verify it on any data if we are good enough at predicting.

Euan Hooper, Boeing Vertol: I'd like to ask the chairman if he has any plans to incorporate this Pitt model in CAMRAD? Wouldn't it be useful for tilt rotor stability?

Johnson: Not for tilt rotors. Tilt rotors, the ones that people are looking at now--not the Boeing design of 15 years ago--but the ones they are doing now, are really low equivalent flap hinge offset, low flap frequency. So they do not generate much in the way of hub moments which is where we really see the large dynamic inflow effects. Most of the stuff that Dave was showing [had] flap frequencies of 1.15 and the like. Really for tilt rotors you only have to worry about the thrust component and it's in axial flight and we've got that one as good as we probably need it. Now probably somebody will design a tilt rotor someday that isn't true about, but right now I don't think that is quite the most important area.

Hooper: But it's in the frequency range isn't it, Dave? Do you agree with Wayne's comment?

Peters: Yes, I guess I have two comments. One in Wayne's defense--if you look at who has come into the dynamic inflow fold through the years--he was one of the first. He has dynamic inflow in CAMRAD and like you say it wouldn't be hard to change that. But remember when you look at the right hand side of the equations it's the aerodynamic component of roll and pitch moment. Even though you've got zero hub moment in roll you've got inertia and aerodynamics that are canceling, right? The inertial moments are pushing on Newton's law, but the aerodynamics parts are pushing on the wake. And that is why Sissingh could find out there was an effect on roll damping even for an articulated blade. Because it's the aerodynamic parts that go on the side. Although somehow for hingeless rotors I think it is bigger than for articulated. But it's still an effect.

Johnson: I think what we are talking about are two different things. The Pitt model is really for forward flight [in the] helicopter mode and in the tilt rotors you will have as much an effect there as you would on any other helicopter. But in axial flight for the tilt rotor you are really back down to momentum theory which does pretty good. There the thrust one is dominant. In support of that I will simply say that I have looked at it. Even the thrust perturbations in dynamic inflow don't seem to matter much in tilt rotor dynamics. I think it's just largely because the other aerodynamics in tilt rotors just overpower things like that.

Jack Landgrebe, United Technologies Research Center: Dave, just so there is no misunderstanding in the audience here, you are talking about dynamic inflow and there is also what we consider variable inflow. You are working with the perturbation inflows required for the stability problem. There is also of course the major area of the actual inflow required to compute the airloads and so forth. In some ways they are connected and in some ways they are two distinct problems. Is there anything that you can glean from the Pitt model that would be helpful in what we call the variable inflow airload prediction sense or do you feel it's strictly applicable to the stability problem?

Peters: I think the latter. I think it's not applicable to loads or things like that. It is a very gross, crude approximation to the induced flow field. In fact, if you look at how it developed, when Dale Pitt first came as my student I said, "Let's take Landgrebe's prescribed wake program and develop the dynamic inflow equations by averaging and getting those gradients." But he did a literature search and anybody that did variable inflow he thought was a candidate-- he has about 150 references in his thesis. And one pulled up this old stuff that he used which was the Kinner distribution. So really we come from you. We've gleaned from those the gems that we needed for dynamic inflow.

Landgrebe: That is what I thought. I had heard from you earlier and I just wanted to make sure there was not a misconception in the audience that the variable inflow problem has been solved through this.

Peters: That is a common misconception, too. A lot of people say, "Wait a minute. People did all those inflow distributions before." They really did and we are thankful they did. We just picked from that the things we needed.